

1 **Crumbs2 is an essential slit diaphragm protein of the**
2 **renal filtration barrier.**

3
4 Annika Möller-Kerutt¹, Juan E. Rodriguez-Gatica², Karin Wacker¹, Rohan Bhatia², Jan-Peter
5 Siebrasse², Nanda Boon³, Veerle Van Marck⁵, Peter Boor⁶, Ulrich Kubitscheck²,
6 Jan Wijnholds^{3,4}, Hermann Pavenstädt¹ and Thomas Weide^{1*}

7
8 ¹) University Hospital of Muenster (UKM), Internal Medicine D (MedD), Albert-Schweitzer-
9 Campus 1 Building A14, 48149 Muenster, Germany

10 ²) Institute of Physical and Theoretical Chemistry; Biophysical Chemistry, Rheinische Friedrich-
11 Wilhelms-University of Bonn, Wegeler Str. 12, 53115 Bonn, Germany

12 ³) Department of Ophthalmology, Leiden University Medical Center (LUMC), Albinusdreef 2,
13 2333 ZA Leiden, The Netherlands

14 ⁴) Netherlands Institute for Neuroscience, Royal Netherlands Academy of Arts and Sciences
15 (KNAW), 1105 BA Amsterdam, The Netherlands

16 ⁵) Gerhard-Domagk Institute of Pathology, University Hospital of Muenster (UKM), Muenster,
17 Germany

18 ⁶) Institute of Pathology, RWTH Aachen University Hospital, Aachen, Germany; Department of
19 Nephrology and Immunology, RWTH Aachen University Hospital, Aachen, Germany

20

1 Supplemental material

2 The supplemental material data consist of three supplemental tables (ST1-3), seven suppl.
3 Figures (SF1-7) and four supplemental video files (SV1-4).

4 Supplemental material table of contents

5 This article contains the following supplemental material:

6

7 Suppl. Tables

8 **Table ST1:** Primers for genotyping and cloning.

9 **Table ST2:** Antibodies used in this study.

10 **Table ST3:** Primer pairs for RT-PCR.

11 **Table ST4:** *Weight of observed wildtype (Cre-) and Crb2^{podKO} (Cre+) mice.*

12 **Table ST5:** *Evaluation of glomerular injury in Crb2^{flox/flox} (control) and Crb2^{podKO} (knockout) mice.*

13 **Table ST6:** *Evaluation of tubular injury in wildtype Crb2^{flox/flox} (Cre-) and Crb2^{podKO} (Cre+) mice.*

14 **Table ST7:** *Localization of CRB2 variants in cells lines.*

15

16 Suppl. Figures

17 **Figure S1:** *Improved spatial resolution by deconvolution.*

18 **Figure S2:** *Crb2 is highly expressed in mice glomeruli.*

19 **Figure S3:** *Non-Mendelian inheritance distribution of Six2-Cre-Crb2^{wt/flox} x Crb2^{flox/flox} breeding.*

20 **Figure S4:** *Analyses of one-week old Crb2^{podKO} and littermate controls.*

21 **Figure S5:** *Crb2 loss results in glomerular sclerosis, accompanied by disordered and effaced foot
22 processes (≥ 8 -weeks-old-mice).*

23 **Figure S6:** *Doxycycline-dependent expression of GFP- or SNAP tagged CRB2.*

24 **Figure S7:** *RNAseq analyses of CRB2 S267A mutant.*

25

26 Suppl. Videos

27 **Video SV1:** SV1_Nephrin_Podocin_3D_overview

28 **Video SV2:** SV1_Nephrin_Podocin_3D_zoom

29 **Video SV1:** SV3_Crb2_Nephrin_3D_overview

30 **Video SV1:** SV4_Crb2_Nephrin_3D_zoom

31

1 Supplemental Tables

2

3 Table ST1: Primers for cloning and genotyping.

4

Cloning			
Target	Species	Direction	Sequence (5'-3')
hCrb2_wt	human	forward	CACCGGGCGCGCCATGGCGCTGGCCAGGCCTGGGAC
hCrb2_wt	human	reverse	TTAATTAACTAGATGAGTCTCTCCTCCGGTGG
hCrb2_S267A	human	forward	GACGAGGACGAGTGTGCAGCCAGCCCCTGCCAGCATGGGGGCCGA
hCrb2_S267A	human	reverse	TCGGCCCCCATGCTGGCAGGGGCTGGCTGCACACTCGTCCTCGTC
hCrb2_N800K	human	forward	GGCGGCAGGCAGTCTCTGGAAGCTCACTGCGGGCTGCGTCTCC
hCrb2_N800K	human	reverse	GGAGACGCAGCCCGCAGTGAGCTTCCAGGACTGCCTGCCGCC
hCrb2_C629S	human	forward	ACTCATTCCGTTCTGACTGTGCC
hCrb2_C629S	human	reverse	GGCACAGTCAGAACGGAAATGAGT
hCrb2_R633W	human	forward	TGCGACTGTGCCTGGCCCCATAGAGG
hCrb2_R633W	human	reverse	CCTCTATGGGGCCAGGCACAGTCGCA
hCrb2_R1249Q	human	forward	ATCCTGGCAGCCCCAAAAGCGCCG
hCrb2_R1249Q	human	reverse	CGGCGCTTTTGGGCTGCCAGGAT
hCrb2_R610W	human	forward	AGAGCAGTGTGGCCTCTGCCTTGTG
hCrb2_R610W	human	reverse	CACAAGGCAGAGGCCAGCACTGCTCT
hCrb2_E792D	human	forward	AGCCAGCCCAGCGACCTCGGGCGGC
hCrb2_E792D	human	reverse	GCCGCCGAGGTCGCTGGGCTGGCT
hCrb2_deltaintra	human	forward	CTGGCAGCCCGAAAGTGACGCCAGTCTGAGGGC
hCrb2_deltaintra	human	reverse	GCCCTCAGACTGGCGTCACTTTCGGGCTGCCAG
NPHS1	human	forward	TTATGTCTCGAGATGGCCCTGGGGACGAC
NPHS1	human	reverse	CTTGCTACCGGTAGCACCAGATGTCCCCTCAGCT
Genotyping			
Target	Species	Direction	Sequence (5'-3')
Crb2Fwd	mouse	forward	TGGAGATGGACAGTGTCTCTC
Crb2Rev	mouse	reverse	GCTCTGGAACAGTCTCCTTG
CreFwd	mouse	forward	GACCAGGTTTCGTTCACTCA
CreRev	mouse	reverse	TAGCGCCGTAAATCAA

5

6

7

1 **Table ST2: Antibodies used in this study.**

2

Protein / Antigen	Species	Manufacturer	Clone, Cat.No	Application
α -Actinin-4	rabbit	Enzo	ALX-210-356	WB (1:1000)
β -Tubulin	mouse	Sigma	T4026	WB (1:1000)
BIP	rabbit	Cell Signaling Technology	C50B12; #3177	WB (1:1000)
Calnexin	mouse	BD Biosciences	Clone 37; 610523	WB (1:1000)
Crb2 (mouse)	rabbit	Jan Wijnholds Group 1) van de Pavert et al., 2004 2) Boroviak et al., 2011		WB (1:500), IF (1:150)
CRB2 (human)	rabbit	Atlas Antibodies	HPA043674	IHC (1:300) WB (1:500)
GFP	mouse	TakaraBio Clontech	JL-8; 632381	WB (1:1000)
Nephrin	guinea pig	Progen	GP-N2	WB (1:500) IF (1:100)
Nephrin	mouse	Santa Cruz	sc-376522	WB (1:500)
Pals1/MPP5	rabbit	ProteinTech	17710-1-AP	WB (1:1000) IF (1:200)
Podocin	rabbit	Sigma	P0372	IF (1:200)

3

4

Protein	Species	Manufacturer	Clone, Cat.No	Application
Anti-rabbit IgG Alexa488	goat	Life technologies	A11034	IF (1:1000)
Anti-rabbit IgG Alexa594	goat	Life technologies	A11012	IF (1:500)
Anti-rabbit IgG Alexa647	goat	Life technologies	A21244	IF (1:500)
Anti-guinea pig IgG Alexa488	goat	Life technologies	A11073	IF (1:500)
Anti-guinea pig IgG Alexa594	goat	Life technologies	A11076	IF (1:500)
Anti-guinea pig IgG Alexa647	goat	Life technologies	A21450	IF (1:500)
HRP-conjugated secondary antibodies	rabbit mouse guinea pig	Dianova; Jackson Immuno Research	-	WB (1:3000)
SNAP-surface® AlexaFluor 488	-	NEB	S9129S	Live cell imaging (1:200, 30 min)
DAPI	-	Roche	-	1:5000

5

6

References

7

8

1) van de Pavert S, Kantardzhieva A, Malysheva A, Meuleman J, Versteeg I, Levelt C, Klooster J, Geiger S, Seeliger M, Rashbass P, Le Bivic A, Wijnholds J (2004) Crumbs homologue 1 is required for maintenance of photoreceptor cell polarization and adhesion during light exposure. *J Cell Sci* 117, 4169-4177

10

11

12

2) Boroviak T, Rashbass P. (2011) The apical polarity determinant Crumbs 2 is a novel regulator of ESC-derived neural progenitors. *Stem Cells* 29:193-205.

13

14

1 **Table ST3:** Primer pairs for RT-PCR.

2

Target	Species	Direction	Sequence (5'-3')
<i>Gapdh</i>	mouse	forward	CCTGGAGAAACCTGCCAAGTA
<i>Gapdh</i>	mouse	reverse	AAGTCGCAGGAGACAACCTG
<i>Crb2</i>	mouse	forward	TGTACCTGCCCTGCCAATTT
<i>Crb2</i>	mouse	reverse	ATGTCAGGCCTGTGTATCCATC
<i>Crb3</i>	mouse	forward	AACGGGGGCCTGTCTTCA
<i>Crb3</i>	mouse	reverse	CCCGAAGTTTTCGCATGAGC
<i>Crb3A</i>	mouse	forward	GCTCATGCGAAAACCTCGGG
<i>Crb3A</i>	mouse	reverse	GGCAGCTTGAGGTTGGGG
<i>Crb3B</i>	mouse	forward	TCCTCCTTATAGCAGTGGGACT
<i>Crb3B</i>	mouse	reverse	CGTGGGAAAACCTGCTCCTCA
<i>Nphs1</i>	mouse	forward	TATCGCCAAGCCTTCACAGG
<i>Nphs1</i>	mouse	reverse	AGCTCAAAGGGCAGAGAACC
<i>Nphs2</i>	mouse	forward	CAGAGGAAGGCATCAAGCCC
<i>Nphs2</i>	mouse	reverse	GGACCTTTGGCTCTTCCAGG
<i>Ccl2</i>	mouse	forward	AGCTGTAGTTTTTGTCAACAAGC
<i>Ccl2</i>	mouse	reverse	TGCTTGAGGTGGTTGTGGAA
<i>Havcr1 (Kim1)</i>	mouse	forward	GCATCTCTAAGCGTGGTTGC
<i>Havcr1 (Kim1)</i>	mouse	reverse	TGCAGCTGGAAGAACCAACA
<i>Lcn2</i>	mouse	forward	ACGGACTACAACCAGTTCCGC
<i>Lcn2</i>	mouse	reverse	AATGCATTGGTCGGTGGGG
<i>Serpine1 (Pai1)</i>	mouse	forward	CACAGGCACTGCAAAAAGGTC
<i>Serpine1 (Pai1)</i>	mouse	reverse	GGATTGTCTCTGTCCGGTTGT
<i>Tagln</i>	mouse	forward	TTATGAAGAAAGCCCAGGAGCA
<i>Tagln</i>	mouse	reverse	TTTGTGAGGCAGGCTAAGCA
Target	Species	Direction	Sequence (5'-3')
<i>GAPDH</i>	human	forward	GGACTCATGACCACAGTCCA
<i>GAPDH</i>	human	reverse	CCAGTAGAGGCAGGGATGATG
<i>B3GALT5</i>	human	forward	CCCCGCGCACGTGAT
<i>B3GALT5</i>	human	reverse	GCCAAGAGGAAATTTGTCTCAAAGA
<i>CANX</i>	human	forward	GATGACTGGGATGAAGATGCC
<i>CANX</i>	human	reverse	CCTCAGGTTTCTCTGCGTCT
<i>CRB2</i>	human	forward	TGTACCTGCCCTGCCAATTT
<i>CRB2</i>	human	reverse	GCCACACACAAAAGCCATC
<i>HSPA5</i>	human	forward	CTCAACATGGATCTGTTCCGGT
<i>HSPA5</i>	human	reverse	ATTCGAGTCGAGCCACCAAC
<i>HYOU1</i>	human	forward	CGGGGAGTAGGATTTGACCG
<i>HYOU1</i>	human	reverse	CGGGGAGTAGGATTTGACCG

3

4

5

6

1 **Table ST4:** Weight of observed wildtype (*Cre*-) and *Crb2*^{podKO} (*Cre*+) mice.

2 The table show the weight of male and female mice used for experiments in this study at different
3 time points. Differences of homozygote (HOM) wildtype (*Cre*-; *Crb2*^{flox/flox}) and mice lacking *Crb2* in
4 podocytes (*Cre*+; *Crb2*^{podKO}) becomes significant after 8 weeks in male and female animals. Statistical
5 evaluation was done by an unpaired two-tailed t-test for comparison of two groups. (n.s.: not
6 significant; * p<0.05)

7

gender	age [weeks]	HOM Cre (-/+)	weight [g]	number of animals	p-value
female	1	-	5.00 ± 0.18	N=4	0.9567 (n.s.)
female	1	+	4.98 ± 0.25	N=4	
male	1	-	4.93 ± 0.23	N=4	0.7369 (n.s.)
male	1	+	4.82 ± 0.17	N=4	
female	5	-	16.06 ± 0.51	N=10	0.0527 (n.s.)
female	5	+	14.97 ± 0.26	N=13	
male	5	-	17.61 ± 0.79	N=6	0.0897 (n.s.)
male	5	+	15.50 ± 0.80	N=7	
female	8	-	20.91 ± 0.78	N=5	0.0446 (*)
female	8	+	17.78 ± 1.06	N=5	
male	8	-	23.66 ± 0.71	N=7	0.0189 (*)
male	8	+	19.97 ± 0.95	N=3	

8

9

1 **Table ST5: Evaluation of glomerular injury in *Crb2*^{flox/flox} (control) and *Crb2*^{podKO} (knockout) mice.**
2 To evaluate glomerular injury, the total amount of glomeruli without, or with segmental (<50%), or
3 global (>50% of the glomerular area) increase in matrix were counted and categorized as “normal”,
4 “segmental glomerular sclerosis” or “global glomerular sclerosis”, respectively. For that more than 70
5 glomeruli of wildtype control mice (*Crb2*^{flox/flox}) and knockout mice that lack *Crb2* in podocytes
6 (*Crb2*^{podKO}) were used (Figure 2 I). This table gives the values as mean injury score, summarizing
7 segmental and global glomerular sclerosis as injury versus normal glomeruli. Values are given in [%] and
8 statistical evaluation was done by an unpaired two-tailed t-test for comparison of two groups. (n.s.:
9 not significant; * p<0.05; ** p<0.01; *** p<0.001)

10

age	mean glomerular injury [%]		p-value
	<i>Crb2</i> ^{flox/flox} control (number)	<i>Crb2</i> ^{podKO} knockout (number)	
5 weeks	3.35 ± 0.89 (N=4)	26.20 ± 1.54 (N=4)	< 0.0001 (***)
8 weeks	2.77 ± 0.66 (N=3)	61.37 ± 5.50 (N=3)	0.0004 (***)

11

12

1 **Table ST6: Evaluation of tubular injury in wildtype *Crb2*^{flox/flox} (Cre-) and *Crb2*^{podKO} (Cre+) mice.**
2 Histopathological analysis: Acute tubular injury was estimated in the corticomedullary areas by
3 determining the percentage of tubules with cast formation, dilatation, and degeneration (including
4 epithelial cell necrosis and loss of apical brush border). For each of these parameters, a five-point scale
5 according to *Marko et al* (JASN, 2016) was used: **0**: normal kidney; **1**: 1%–25%; **2**: 25%–50%; **3**: 50%–
6 75%; **4**: 75%–100% tubular injury. The table gives the mean injury score for the different kind of tubular
7 alterations (cast formation, dilatation of tubules and tubular degeneration). For each animal (N≥3) n≥
8 5 visual fields were evaluated. Statistical evaluation was done by an unpaired two-tailed t-test for
9 comparison of two groups. (n.s.: not significant; * p<0.05; ** p<0.01)

10

age	type of tubular injury	mean injury score [%]		p-value
		<i>Crb2</i> ^{flox/flox} control (number)	<i>Crb2</i> ^{podKO} knockout (number)	
5 weeks	cast	0.04 ± 0.04 (N=3)	0.07 ± 0.04 (N=4)	0.6623 (n.s.)
5 weeks	dilatation	0.16 ± 0.11 (N=3)	0.92 ± 0.22 (N=4)	0.0388 (*)
5 weeks	degeneration	0.04 ± 0.04 (N=3)	0.46 ± 0.19 (N=4)	0.1046 (n.s.)
8 weeks	cast	0.03 ± 0.03 (N=4)	1.48 ± 0.44 (N=4)	0.0165 (*)
8 weeks	dilatation	0.28 ± 0.15 (N=4)	2.27 ± 0.48 (N=4)	0.0076 (**)
8 weeks	degeneration	0.03 ± 0.03 (N=4)	2.42 ± 0.74 (N=4)	0.0180 (*)

11

12

1 **Table ST7: Localization of CRB2 variants in cells lines.**

2 The number of cells expressing CRB2-EGFP variants localized at the cell surface/plasma membrane or
 3 intracellularly, at the ER (*endoplasmic reticulum*) was determined for immortalized podocyte (AB8) and
 4 HEK293T cell lines. More than 200 cells per EGFP-CRB2 expressing variant were analyzed for stable
 5 AB8 based cell lines.

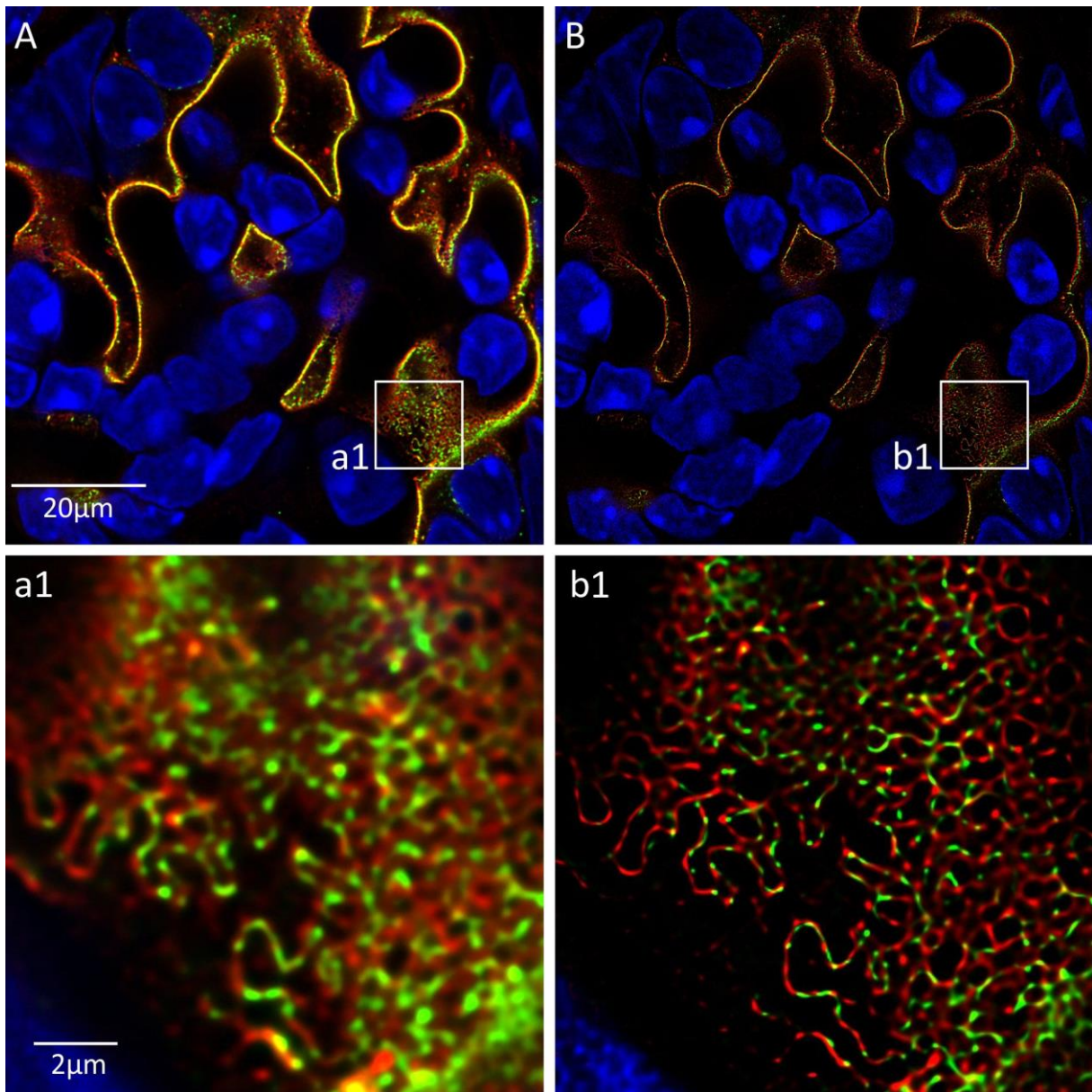
CRB2 variant (mutant)	cell line	PM localization [%]	ER localization [%]	Disease-associated	remarks
WT	AB8	96.0	4.0	no	(wildtype)
S267A ¹⁾	AB8	2.3	97.7	no	mutant according to (Ramkumar et al., 2015)
R610W	AB8	94.0	6.0	no	evaluated as benigne
C629S	AB8	3.4	96.7	yes	Ebarasi et al., 20015
R633W	AB8	7.5	92.5	yes	Slavotinek et al., 2015
E792D	AB8	94.8	5.2	no	evaluated as benigne
N800K	AB8	14.0	86.0	yes	Slavotinek et al., 2015
R1249Q ²⁾	AB8	10.7	89.3	yes/unclear	Ebarasi et al., 2015/ uncertain significance (ClinVar)

6 ¹⁾ mutant S267A inactivates putative conserved O-glycosylation for POGlut by changing serin into alanine.

7 ²⁾ Homozygous CRB2 R1249Q variants have been linked to SRNS-like phenotype, FSGS9 (Ebarasi et al., 2015) and was
 8 interpreted as "pathogenic". Two latter submissions observed no phenotype in homozygous humans and interpreted
 9 R1249Q homozygosity as "benign" (submission 2019, Dec, 31th by Invitae) or of "uncertain significance" (submission
 10 2020, Jan, 6th by Reproductive Health Research and Development, BGI Genomics). Source:
 11 <https://www.ncbi.nlm.nih.gov/clinvar/variation/180703>
 12

1 Supplemental Figures

2



3

4

5 **Figure S1:** *Improved spatial resolution by deconvolution.*

6 **(A)** A single image of a glomerulus stained against Nephtrin (green), Podocin (red) and DAPI (blue). The

7 sample was imaged with a Leica SP8 using a 40x/1.1 water objective. Lateral size, 80.3 x 80.3 µm². **(B)**

8 Image after the deconvolution process **(a1-b1)** The magnifications demonstrate that an improved spatial

9 resolution was obtained by the deconvolution process allowing the visualization of details that

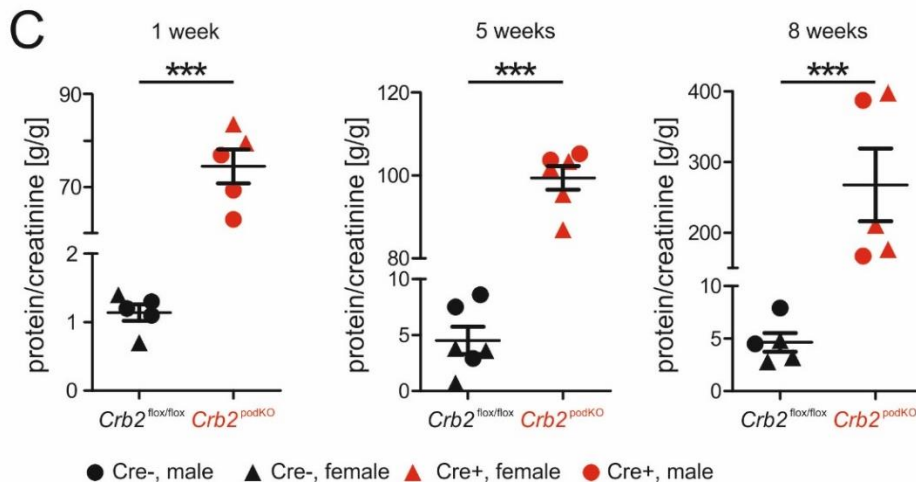
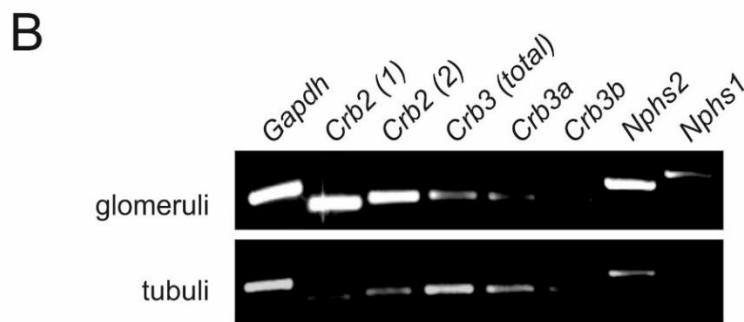
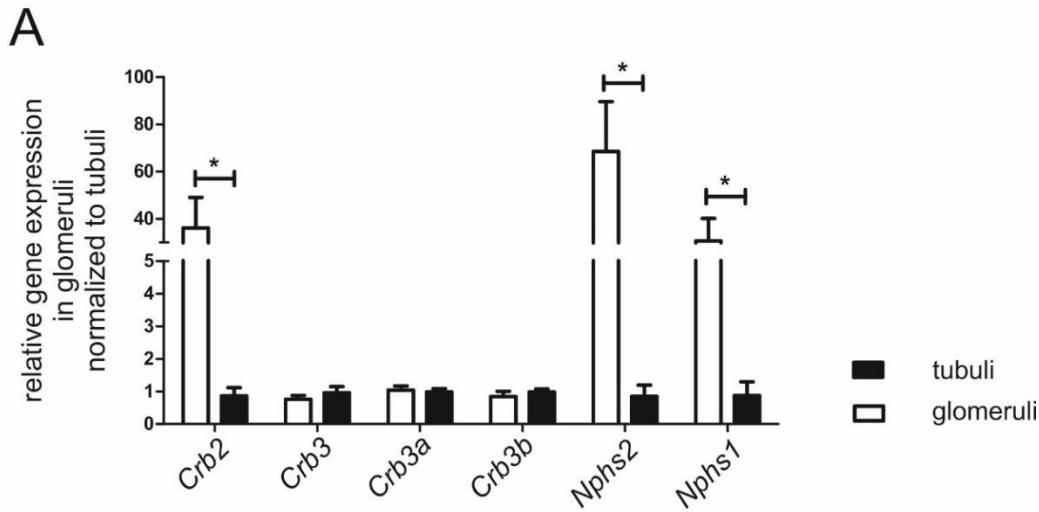
10 elucidated similar but slightly separated patterns of the Nephtrin and Podocin signals. The same applied

11 to the Crb2/Nephtrin stained samples.

12

13

14



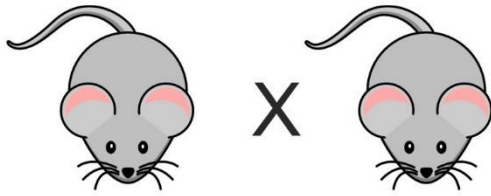
1 ● Cre-, male ▲ Cre-, female ▲ Cre+, female ● Cre+, male

2

3 **Figure S2: *Crb2* is highly expressed in mice glomeruli.**

4 **(A)** Relative gene expression (qRT-PCR analysis) of *Crb2* in comparison to isoforms *Crb3a* and *Crb3b* and
5 SD markers *Nphs1* (Nephrin) and *Nphs2* (Podocin) in murine glomeruli normalized to the tubular
6 fraction. **(B)** Representative corresponding agarose gel of used primers pairs in RT-PCR experiments. **(C)**
7 Quantification of proteinuria by determination of the protein creatinine ratio, indicating male circles)
8 and female (triangles) mice. (N=5, per group). Unpaired two-tailed t-Test: * p<0.05; ** p<0.01;
9 *** p<0.001

$Crb2^{flx/flx}$ $Six2-Cre, Crb2^{wt/flx}$



		$Crb2^{flx/flx}$	
		homozygous	heterozygous
Six2 Cre	positive	0	10
	negative	5	9

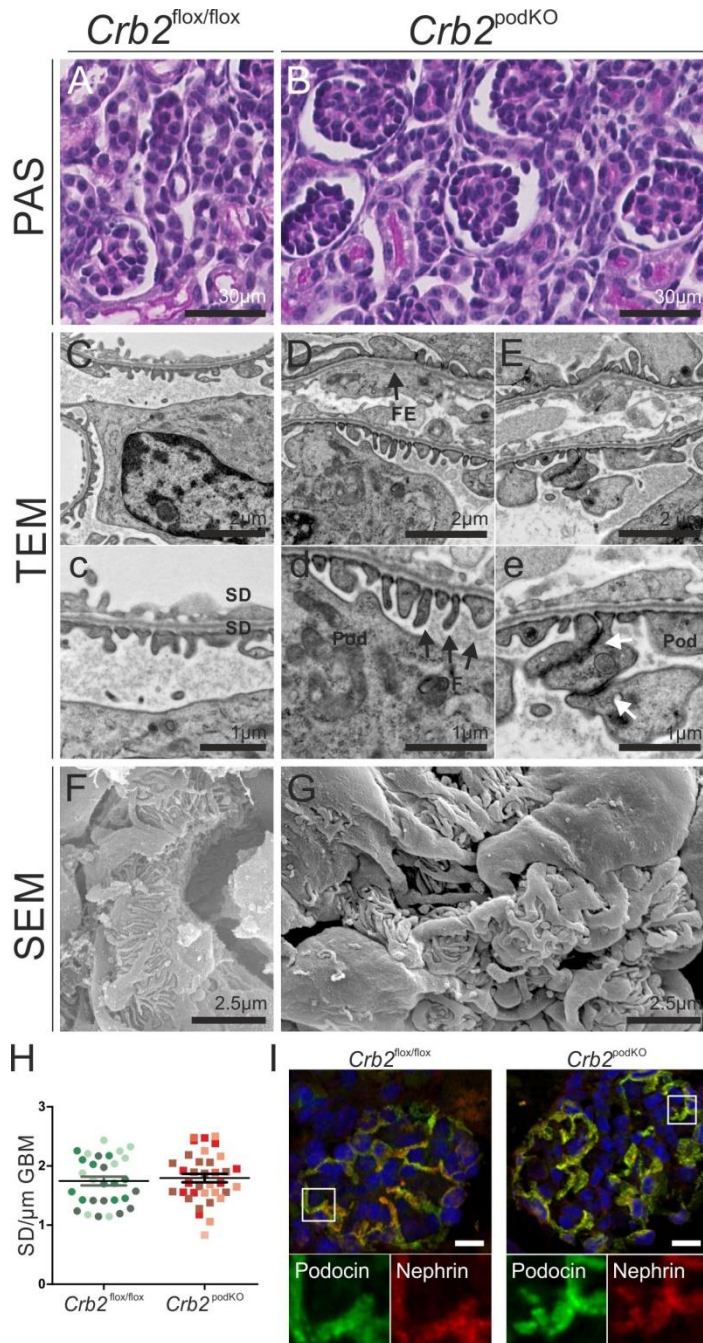
1

2

3 **Figure S3: Non-Mendelian inheritance distribution of $Six2-Cre-Crb2^{wt/flx}$ x $Crb2^{flx/flx}$ breeding.** Breeding
 4 of heterozygous Six2-Cre positive, $Crb2^{wt/flx}$ with $Crb2^{flx/flx}$ should result in in the following Mendelian
 5 ratios: 25% $Crb2^{wt/flx}$; 25% $Crb2^{flx/flx}$ (both Six2 Cre-negative); 25% Six2-Cre; $Crb2^{wt/flx}$; 25% Six2-Cre;
 6 $Crb2^{flx/flx}$ (both Six2-Cre positive). F1 mice that totally lack Crb2 (homozygote $Crb2^{flx/flx}$ Six2-Cre
 7 positive; $Crb2^{six2KO}$) offspring are missing, suggesting $Crb2^{six2KO}$ result in embryonic lethality.

8

1



2

3

4 **Figure S4: Analyses of one-week old *Crb2*^{podKO} and littermate controls.**

5 **(A,B)** PAS staining: Kidney tissue of one-week-old *Crb2*^{podKO} showed no obvious difference between

6 *Crb2*^{flox/flox} and *Crb2*^{podKO} mice. **(C-E)** TEM analyses: Ultrastructural analyzes revealed some foot process

7 effacement (FE, arrow) and processes of different sizes (D,d) in comparison to littermate control mice

8 (C,c). In addition, podocytes of *Crb2*^{podKO} showed electron-dense regions between the cells (E, e; white

9 arrows). **(F,G)** SEM analyses of the wildtype (F) and *Crb2*^{podKO} mice (G). **Pod**: podocyte cell body, **FE**: foot

10 process effacement, **DF**: disordered foot process **(H)** Slit diaphragm (SD) number per μm GBM is not

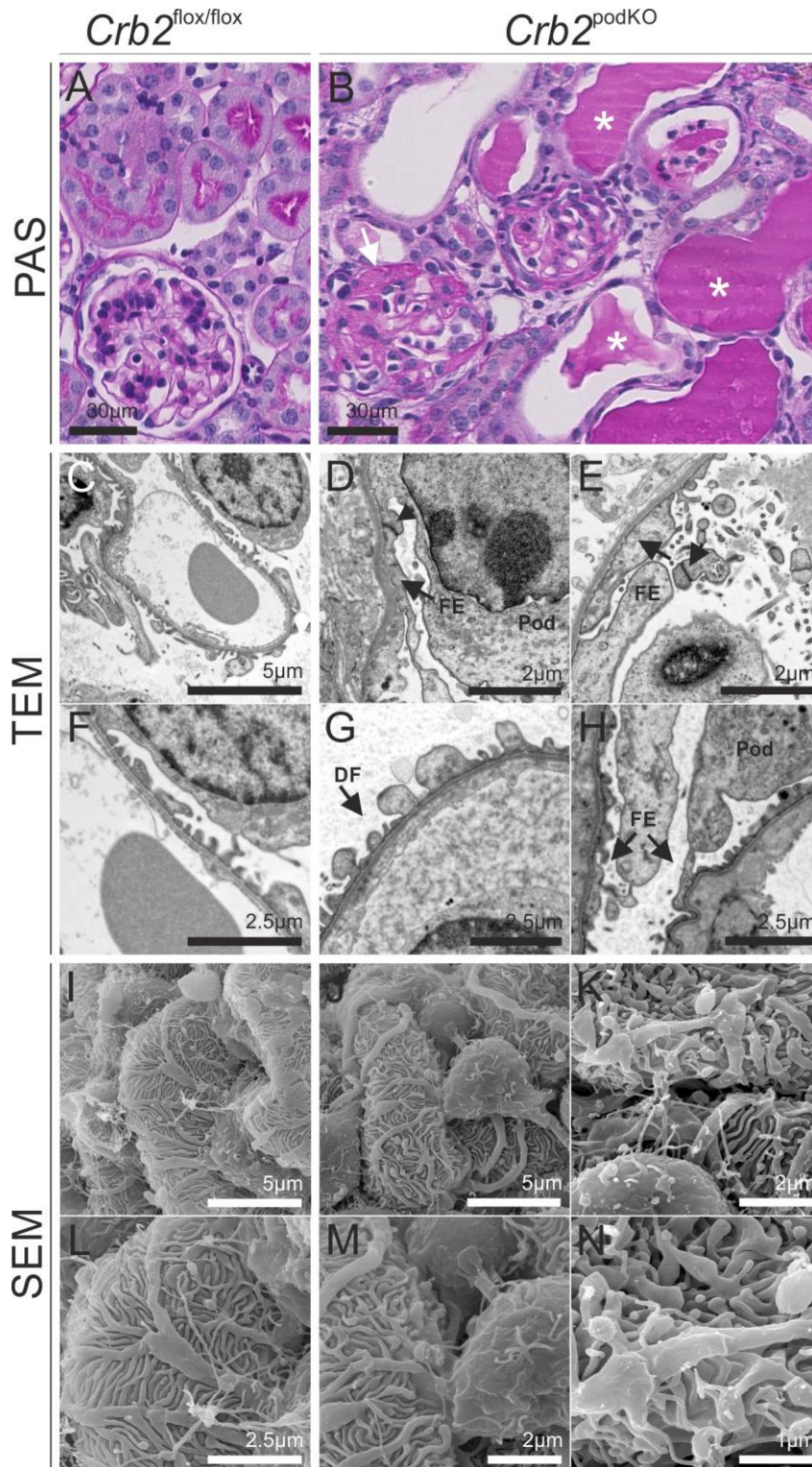
11 altered in 1-week old *Crb2*^{podKO} animals (N=3, >250 μm GBM). **(I)** Illustrative immunofluorescence

12 analyses of SD-proteins Nephrin (red) and Podocin (green) in glomeruli from *Crb2*^{flox/flox} and *Crb2*^{podKO}

13 show similar staining pattern at this age.

14

1

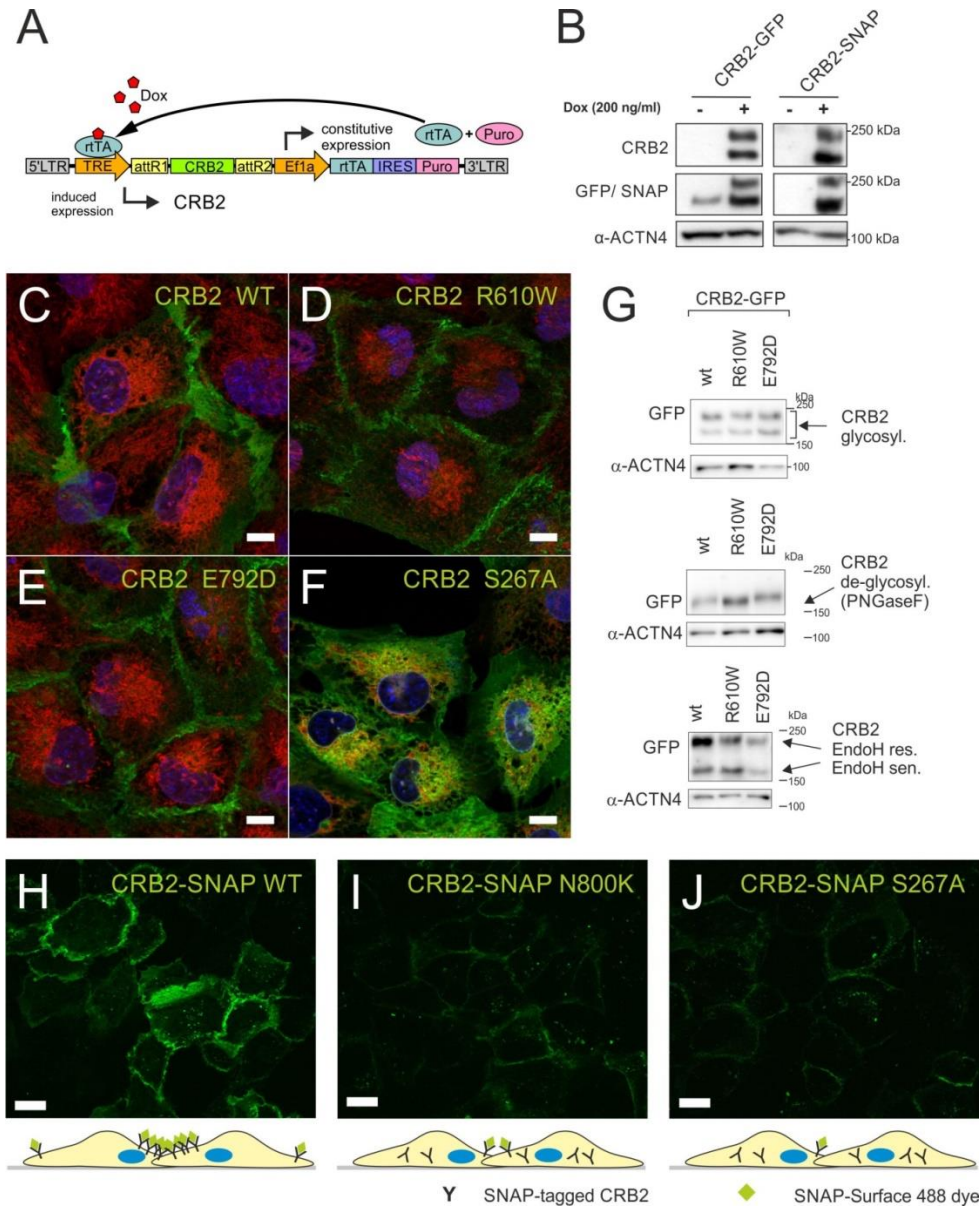


2

3 **Figure S5:** *Crb2* loss results in glomerular sclerosis, accompanied by disordered and effaced foot
 4 processes (≥ 8 -weeks-old mice).

5 **(A,B):** PAS staining: The wildtype mice showed typical tubular and glomerular structures. Glomeruli of
 6 *Crb2*^{podKO} showed segmental sclerosis (white arrow). Renal tubuli were dilated and contained protein
 7 casts (white asterisks) **(C-H):** TEM analyses: Ultrastructural analyzes revealed increased foot process
 8 effacement (FE arrow) and processes of different size (G,H) in comparison to littermate controls (C,F).
 9 **(I-N)** SEM analyses: By contrast to the wildtype (I,L) podocytes foot processes of *Crb2*^{podKO} mice were
 10 disordered, of variable size (J,K) and developed rounded ends (M,N).

11 **Pod:** podocyte cell body, **FE:** foot process effacement, **DF:** disordered foot process



2

3

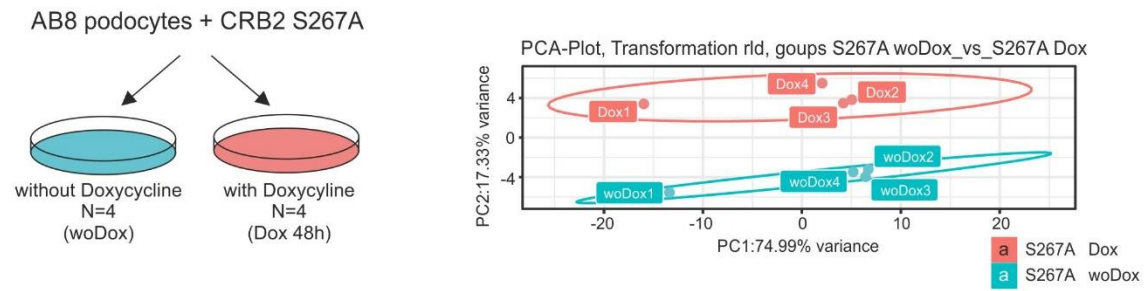
4 **Figure S6: Doxycycline-dependent expression of GFP- or SNAP tagged CRB2.**

5 (A) Scheme: The lentiviral pINDUCER21_Puro system was used to express various CRB2 wildtype as well
 6 as CRB2 mutants and variants under the control of doxycycline (Dox). (B) Western blot: Stable AB8
 7 podocyte cell lines express GFP- or SNAP tagged CRB2 only after administration of Dox (200ng/ml).
 8 Expression was validated with antibodies against CRB2 or against the used GFP and SNAP tags,
 9 respectively. AB8 cells have no endogenous CRB2 expression. (C-F) We added two non-pathogenic CRB2
 10 variants (R610W and E792D) to our studies. CRB2 R610W and E792D variants showed a clear localization
 11 in overlapping regions, similar as the used CRB2 wildtype (The CRB2 S267A mutant served was included
 12 to show non-surface localization). (G) R610W and E792D showed same glycosylation pattern in
 13 glycosylation analyses as the used CRB2 wildtype. (H-J) Surface labeling assays of SNAP-tagged Crb2
 14 wildtype and N800K and S267A mutants in combination with the cell membrane impermeable SNAP-
 15 Surface[®] 488 dye. Only SNAP-tags on the surface of cells are able to bind the surface labeling dye.
 16 Compared to the WT protein (H) N800K (I) and S267A (J) Using identical exposure times, Crb2 mutants
 17 strongly showed a strongly reduced surface labeling in comparison to strongly positive CRB2 wildtype.
 18 Scale bar= 10 μ m.

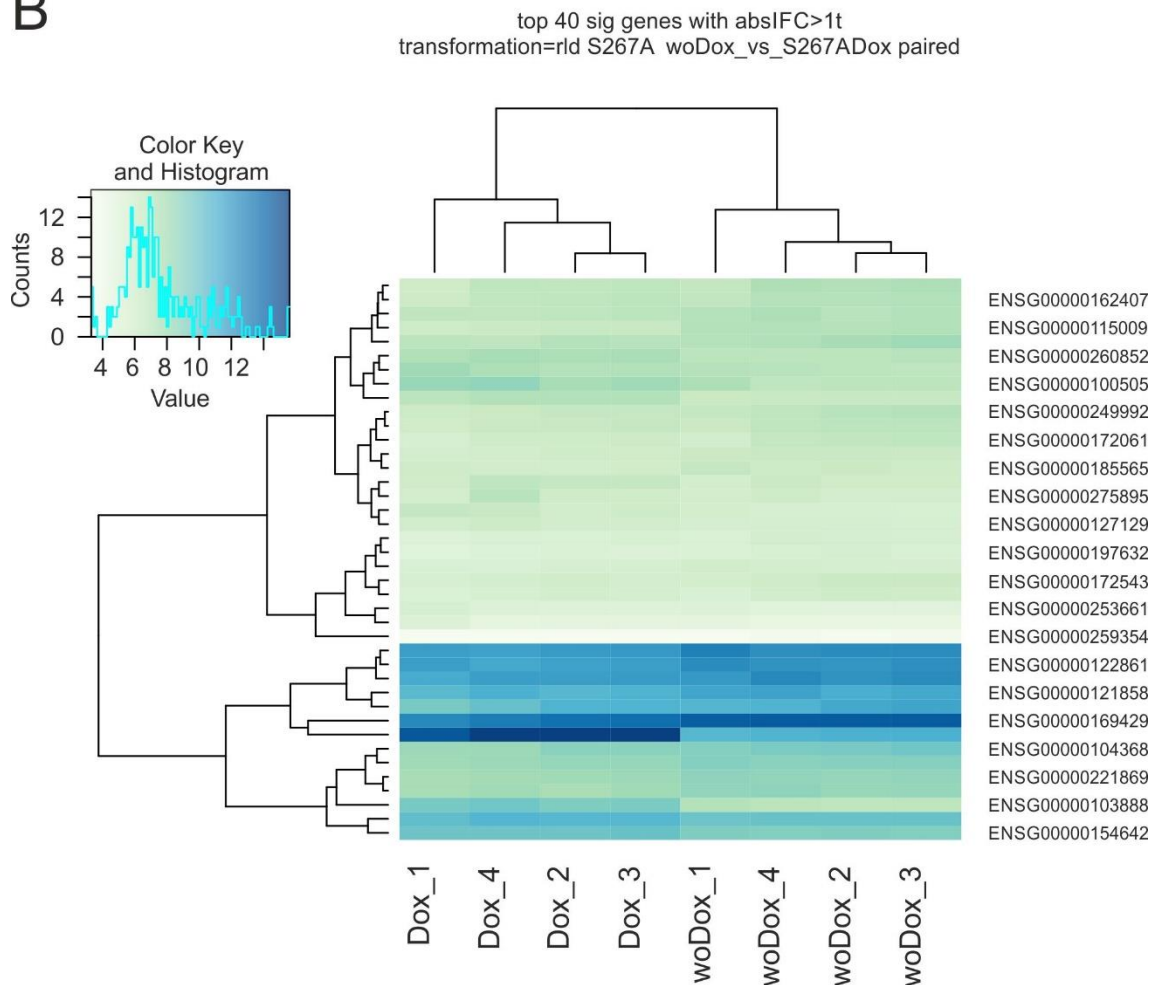
19

20

A



B



1

2 **Figure S7:** RNAseq analysis of CRB2 S267A mutant.

3 **(A) left:** Setup of RNAseq analyses of AB8 podocyte cells expressing the GFP-tagged S267A Crb2 mutant
 4 (with Doxycycline, Dox) compared to non-induced control (woDox); **right** PCA-Plot transformation of
 5 the used samples of AB8 cells without (woDox) and with doxycycline induced (Dox) overexpression of
 6 Crb2-GFP S267A (N=4). **(B)** Heatmap of rlog-transformed values across samples of the top 40 significant
 7 regulated genes emphasizes the clear separation of four induced (Dox) and four non-induced (woDox)
 8 samples.

9

1 Supplemental Videos

2 **Video SV1:** *SV1_Nephrin-Podocin_3D_overview_720_20_fps*

3 3D stack of an expanded glomerulus stained against Nephrin (green), Podocin (red) and DAPI (blue).
4 Sample imaged with a Leica SP8. Size 80.3. x 80.3 x 16.9 μm^3 (63 slices, 40x/1.1 NA water objective). The
5 sample is shown after deconvolution with Huygens using the CLME algorithm, SNR: 40. The video
6 highlights the Nephrin/Podocin structures first in a 3D rendering done with Imaris software and shows
7 later the nuclei stained with DAPI to give a better representation of the spatial distribution.

8

9 **Video SV2:** *SV1_Nephrin-Podocin_3D_zoom_720_20_fps*

10 3D segmentation of a region of an expanded glomerulus showed in the supplementary video **SV1**,
11 visualizing that the intracellular adapter Podocin (red) localizes more closely to the nuclei (blue) than
12 the transmembrane protein Nephrin (green). Segmentation was performed in Imaris using the Surface
13 tool, independently on each channel, considering a bounding box of 23. x 19.6 x 10 μm^3

14

15 **Video SV1:** *SV3_Crb2-Nephrin_3D_overview_720_20_fps*

16 3D stack of an expanded glomerulus stained against Crb2 (green), Nephrin (red) and DAPI (blue). The
17 sample was imaged with a Leica SP8. Size 90.7. x 90.7 x 24.1 μm^3 (105 slices, 40x/1.1 NA water objective).
18 The sample is shown after deconvolution with Huygens using the CLME algorithm, SNR: 40. The video
19 highlights the Crb2/Nephrin structures first in a 3D rendering done with Imaris and showing later the
20 nuclei stained with DAPI to give a better representation of the spatial distribution.

21

22 **Video SV1:** *SV4_Crb2-Nephrin_3D_zoom_720_20_fps*.

23 3D segmentation of a region of an expanded glomerulus showed in the supplementary video **SV2**,
24 revealing the presence of adjacent Crb2 (green) and Nephrin (red) clusters, in contrast to the
25 Nephrin/Podocin localization. Segmentation was performed in Imaris using the Surface tool,
26 independently on each channel, considering a bounding box of 23. x 19.6 x 10 μm^3

27